Theor Chem Acc (2012) 131:1232
DOI 10.1007/s00214-012-1232-9

REGULAR ARTICLE

Proton exchange reactions of C2–C4 alkanes sorbed in ZSM-5 zeolite

Kanjarat Sukrat · Daniel Tunega · Adelia J. A. Aquino · Hans Lischka · Vudhichai Parasuk

Received: 3 March 2012 / Accepted: 2 May 2012 / Published online: 30 May 2012

Abstract An extensive theoretical study has been carried out to determine barriers for the proton exchange reactions of C2–C4 alkanes in ZSM-5. It was found that cluster size and cavity structure are very important for predicting this barrier. A decrement of up to 20 kcal/mol was observed when employing the periodic model instead of using the small cluster model. Effects of basis set quality and electron correlation to the activation energy are positive and in combination could contribute up to 8 kcal/mol. An extrapolation scheme for estimating the reaction barrier that takes into account effects of cluster size, basis set quality, and electron correlation has been proposed. The regioselectivity and the chain length were discussed.

Keywords ZSM-5 zeolite · Proton exchange · Density functional theory · Activation barrier

Dedicated to Professor Marco Antonio Chaer Nascimento and published as part of the special collection of articles celebrating his 65th birthday.

K. Sukrat · V. Parasuk
Department of Chemistry, Faculty of Science, Chulalongkorn University, Phyathai Rd., Pathumwan, Bangkok 10330, Thailand

D. Tunega · H. Lischka (✉)
Institute of Theoretical Chemistry, University of Vienna, Währingerstraße 17, 1090 Vienna, Austria
e-mail: hans.lischka@univie.ac.at

D. Tunega · A. J. A. Aquino
Institute of Soil Research, University of Natural Resources and Life Sciences, Peter-Jordan-Straße 82, 1190 Vienna, Austria

A. J. A. Aquino · H. Lischka
Department of Chemistry and Biochemistry, Texas Tech University, Lubbock, TX 79409-1061, USA

1 Introduction

Currently, the fluid catalytic cracking (FCC) represents the largest volume of catalysts used in oil refineries. From 2008 to 2011, the catalytic cracking consumption was forecast to increase from 919 to 998 million US dollar [1–3]. The catalytic cracking process involves 3 basic reactions such as proton exchange ($Z^-H_B^+ + C_nH_{2n+2} \rightarrow Z^-H^+ + C_nH_{2n+1}H_B$), C–C bond cleavage ($Z^-H_B^+ + C_nH_{2n+2} \rightarrow Z^-C_{(n-x)}H_{2(n-x)+1}^+ + C_xH_{2x+1}H_B$), and dehydrogenation ($Z^-H_B^+ + C_nH_{2n+2} \rightarrow Z^-C_nH_{2n+1}^+ + HH_B$). The competition between these reactions determines the ratio of petrochemical products. Thus, the knowledge and predictability of these reactions are valuable. Many experimental studies have been carried out for the proton exchange reactions of small and large alkanes with the Brønsted acid site of zeolites [4–10]. However, the mechanism of the proton exchange reaction is far from conclusive. Two mechanisms, direct [11] and mediated [12] proton exchange, have been proposed. The direct mechanism is a single-step mechanism involving a direct transfer of the Brønsted acidic proton (H_B^+) from a zeolitic framework to the alkane molecule. The mediated mechanism involves two proton transfer steps. In first step, H_B^+ transfers to an alkene molecule (representing an impurity in the alkane sample). The second step involves the transfer of hydride ion from a nearby alkane to the alkyl cation. Generally, there are 3 carbon positions in alkanes for the H-exchange reaction with the Brønsted proton of zeolites. These positions will be referred to as primary, secondary, and tertiary, respectively. It was also found that there exists

the regioselectivity in the proton exchange reaction of small alkanes [10, 13]. For example, the proton exchange rate at the primary position of propane was reported to be 1.5 times faster than at the secondary position [7]. Theoretical studies play an important role in the elucidation of the mechanism and the explanatory of the regioselectivity of the proton exchange reaction of alkanes. Zimmerman et al. [14] have suggested for the density functional theory (DFT) calculations that using large clusters of zeolite framework combining with a proper dispersion functional gives results in a good agreement with experimental results. They also found that in the larger clusters, the lower of energy barrier is a result from the effects of the electrostatic stabilization in cracking transition-state structures (TSs) and the long-range interactions, whereas both effects are missed in the small cluster models. A large number of theoretical works have been carried out in this light [15–19]. However, due to the size of zeolites, small-size cluster model (3T or 5T models where T represents alumina or silica tetrahedron) has been employed in most of those studies. The small-size cluster model could not appropriately describe the effect of the zeolites' porous structure or cavity toward the reactivity or selectivity of the catalyst. Recently, Bučko et al. [20] have carried out calculations on periodic models using PW91 with plane wave basis set and molecular dynamics simulations for the proton exchange reaction of small alkanes in chabazite. They concluded that the entropic effect is an important driving force for the regioselectivity of the proton exchange reaction of small alkanes and that *iso*-butane (*i*-butane) proceeds through the mediated mechanism, while for other alkanes, the direct mechanism is preferred. However, their calculations were performed in chabazite, zeolite with significantly smaller cavities than in the commercial and widely used catalyst ZSM-5.

In this work, the proton exchange reactions of four small alkanes, that is, ethane, propane, *i*-butane, and normal-butane (*n*-butane), in ZSM-5 were studied by means of quantum chemical methods. Effects of the size of the cluster model, the quality of basis set, and the importance of the level of electron correlation were systematically investigated. The proton exchange barriers and the regioselectivity of these alkanes sorbed in ZSM-5 were addressed. The summary of types of proton exchange reactions of studied alkanes is given in Table 1.

Table 1 Types of proton exchange reactions of C2–C4 alkanes, with notation for further reference given in parenthesis

Alkanes	Types of proton exchange reaction
Ethane	Primary (ethane)
Propane	Primary (propane/1); secondary (propane/2)
Iso-butane	Primary (*i*-butane/1); tertiary (*i*-butane/3)
Normal-butane	Primary (*n*-butane/1); secondary (*n*-butane/2)

2 Computational details

2.1 Models of ZSM-5 and optimizations

Coordinates of ZSM-5 were taken from crystallographic data of silicalite-1 [21], and then, the Si atom at the intersection between the straight and sinusoidal (zigzag) channel (T7) was replaced by the Al atom. This single substitution provides a Si/Al ratio of 95. An acidic proton associated with the substitution was also added to one of the O atoms adjacent to the Al to balance the negative charge. Five cluster models, 5T, 20T, 28T, 38T, and 96T, were employed. The 96T model contains the whole ZSM-5 unit cell. In the 5T model, oxygen atoms at its edge (Si–O bonds) were saturated with hydrogen atoms. In case of the 20T, 28T, 38T, and 96T models, oxygen atoms at their edge were replaced by H atoms. Directly from the crystal lattice, the silicate components were locally fixed and there is no change even after substitution with other parts. In addition, the periodic model denoted as P was also considered. The periodic model was created from the unit cell of ZSM-5 obtained from crystallographic data [21]. Illustrations of five cluster models (5T, 20T, 28T, 38T, and 96T) and the periodic model are given in Fig. 1.

For the 5T, 20T, 28T, and 38T clusters, geometry optimizations of alkanes, isolated clusters, reactant/product complexes (Rcx), and TS were performed using two approaches—RI-PBE/SVP (the Turburmole program's [22] implementation of the resolution of identity integral approximation (RI) [23] in DFT with the Perder–Burke–Ernzerhof functional [24, 25] and the SVP basis set [26–28]) and PBE/DNP [29–31] (Dmol3 program [21] implementation of PBE functional and the double numerical (DN) basis set plus polarization), respectively. Partial geometry optimization was performed by relaxing the acid site and O–H terminals for the 5T cluster model, while for the 20T, 28T, and 38T clusters, Si–H terminals were fixed. For both reactant complexes and transition-state structures, only positions of atoms involved in the reaction were optimized, while positions of atoms in the zeolite skeleton were fixed. For 96T and P models, optimized structures of Rcx with alumina tetrahedron were acquired in a similar manner to that of the smaller cluster but using PBE/DNP. While the structures of TS were obtained by performing single-point calculations on structures generated by embedding TS structures of 38T to 96T and P models. Frequency calculations were carried out on optimized structures of bare clusters, alkanes, and TS for 5T, 20T, 28T, and 38T using RI-PBE/SVP.

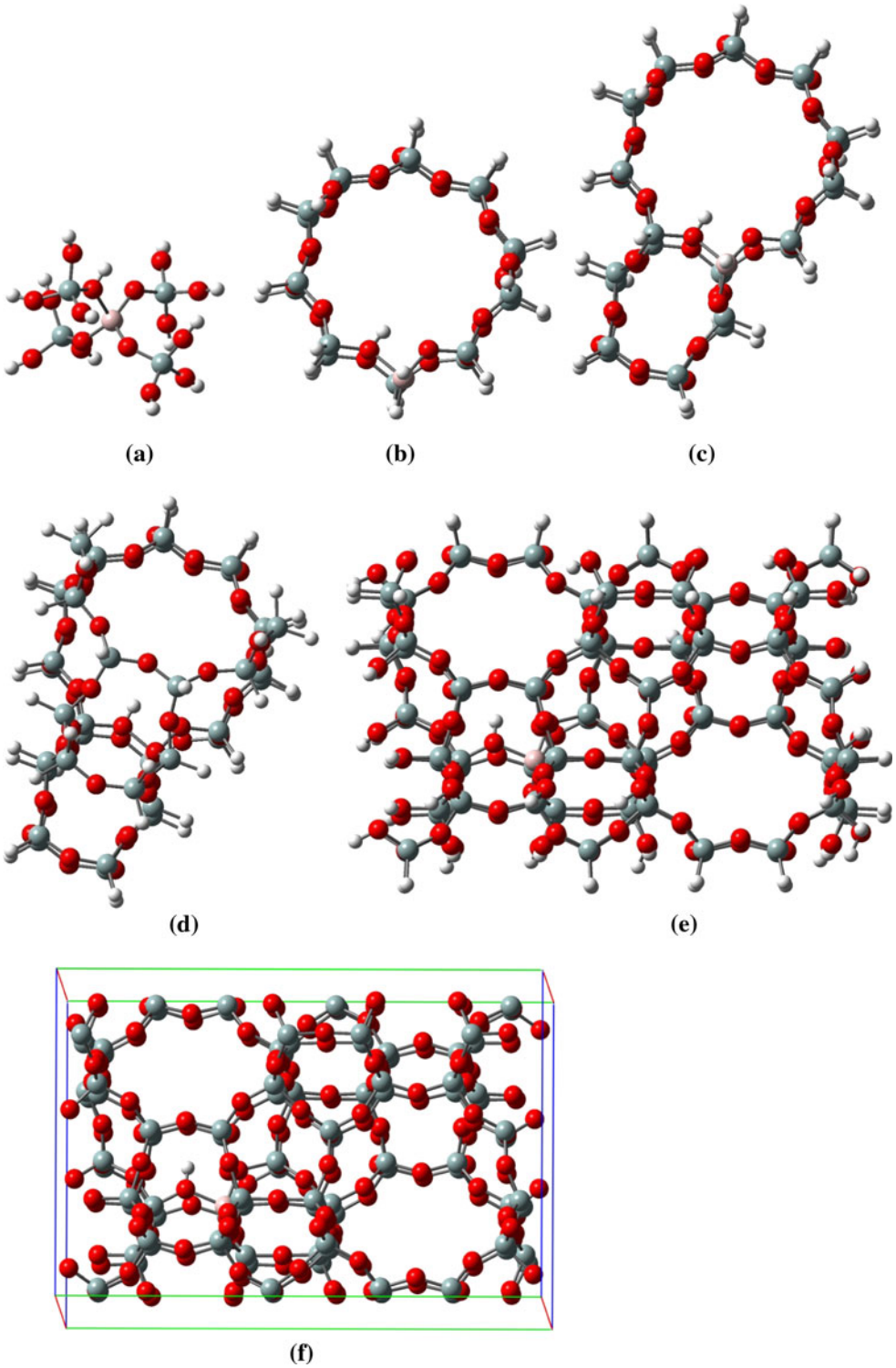

Fig. 1 Illustration of cluster models used in this study. **a** 5T, **b** 20T, **c** 28T, **d** 38T, **e** 96T; **f** periodic model

2.2 Adsorption energy and reaction barrier

Figure 2 described relations between adsorption energy (E_{ads}) and reaction barrier ($\Delta E^{\ddagger}$). The E_{ads} of C2–C4 alkanes in ZSM-5 were calculated according to

$$\text{ZSM-5} + C_nH_{2n+2} \rightarrow \text{ZSM-5} \cdots C_nH_{2n+2}.$$

Therefore,

$$E_{ads} = E(\text{ZSM-5}) + E(\text{alkane}) - E(\text{Rcx}) \quad (1)$$

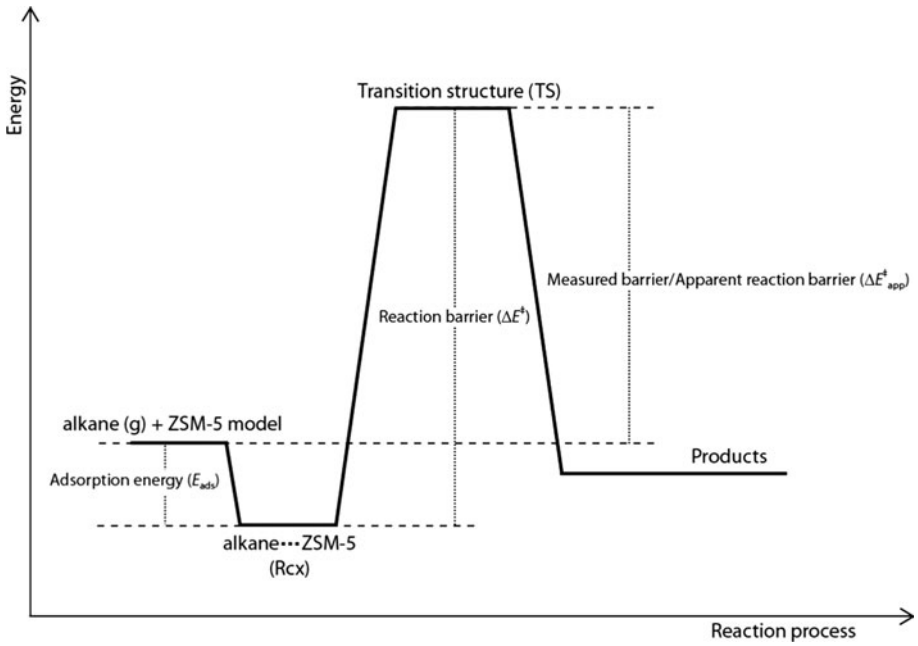

Fig. 2 Energy diagram for proton exchange reaction of alkanes C2–C4

where E(Rcx) is the energy of the reactant complex, E(ZSM-5) is the energy of the bare ZSM-5 structural model, and E(alkane) is the energy of the free alkane molecule.

The (intrinsic) reaction barrier ($\Delta E^{\ddagger}$) of the proton exchange reaction was calculated according to

$$\text{ZSM-5}\cdots\text{C}_n\text{H}_{2n+2} \rightarrow \text{ZSM-5}\cdots\text{C}_n\text{H}^{\ddagger}_{2n+2}$$

and thus

$$\Delta E^{\ddagger} = E(\text{TS}) - E(\text{Rcx}) \tag{2}$$

where E(TS) is the energy of the transition state.

The apparent reaction barrier ($\Delta E^{\ddagger}_{\text{app}}$), the value which is comparable to the measured activation energy, is therefore defined as

$$\Delta E^{\ddagger}_{\text{app}} = \Delta E^{\ddagger} - E_{\text{ads}} \tag{3}$$

Since E_{ads} according Eq. (1) is positive, $\Delta E^{\ddagger}_{\text{app}}$ is always smaller than $\Delta E^{\ddagger}$.

2.3 Complete basis set (CBS) extrapolation

To evaluate the effect of basis set, an extrapolation to the complete basis set (CBS) limit at MP2 and PBE levels of theory has been performed according to the scheme suggested by Helgaker et al. [32]

$$E_X = E_\infty + AX^{-\alpha} \tag{4}$$

where the cardinal number $X = 2$, 3, and 4 is corresponding to the SVP, TZVPPP, and QZVPP basis set, respectively. To obtain α and A, we carried out MP2 and PBE calculations for reactant complexes of ethane, propane, *n*-butane, and *i*-butane with the 5T model.

From our RI-PBE calculations, we found that various reactant complexes between alkanes and ZSM-5 have very similar value for α and the value of 6.56 gave the best fit. A similar observation could also be noticed for RI-MP2 calculations. In addition, there has been a report [23] that the α value depends mainly on method and basis set and it does not vary much for the molecular system with the same set of atoms. Thus, values of α from RI-PBE and RI-MP2 calculations were later used to determine CBS limit at 38T model through Eq. (5) proposed by Truhlar et al. [23].

$$E_\infty = \left(\frac{3^\alpha}{3^\alpha - 2^\alpha}E_3 - \frac{2^\alpha}{3^\alpha - 2^\alpha}E_2\right) \tag{5}$$

3 Results and discussions

3.1 Transition-state structures

The transition state (TS) of the proton exchange reaction of alkanes in ZSM-5 involves the formation of the pentacoordinated carbonium ion. Therefore, a single-step or direct mechanism is suggested. The example of the TS structure of the proton exchange reaction (5T model) is shown in Fig. 3.

Selected geometrical parameters for the TS structures of the 38T cluster model are provided in Table 2. Considering the TS structures for the reaction at the primary carbon (C_1) and C_1–H^{+}_{B}, C_1–H distances are 1.282 and 1.289 Å for ethane, 1.278 and 1.286 Å for propane, 1.285 and 1.282 Å for *n*-butane/1, and 1.283 and 1.271 Å for *i*-butane/1.

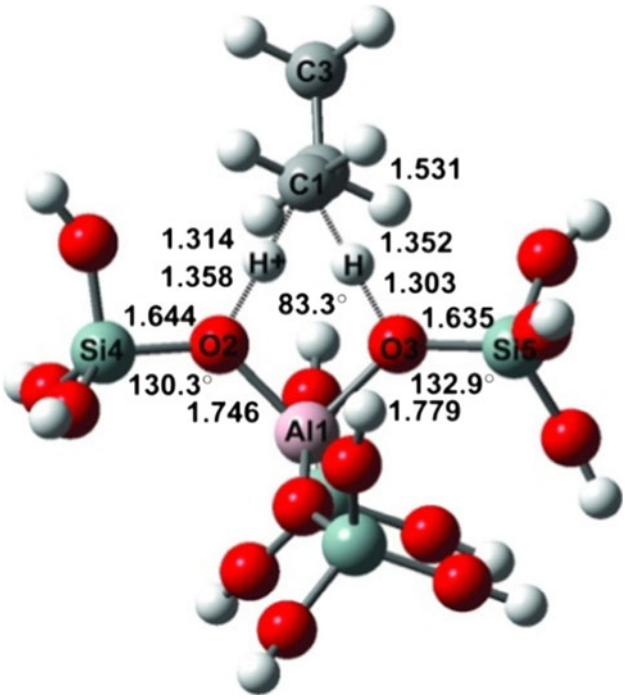

Fig. 3 The transition-state structure with selected geometrical parameters of the proton exchange reaction in propane/1

Apparently, the C1–H_B^+ and C1–H distances at the primary position are almost equal. For the proton exchange reaction on the secondary carbon (C_2), the C_2–H_B^+ distance in the transition state is shorter than C_2–H distance, that is, 1.251 and 1.338 Å for propane/2, and 1.249 and 1.331 Å for *n*-butane/2. For the reaction at the tertiary position (C_3) of *i*-butane/3, it is observed that C_3–H_B^+ is longer than the C_3–H distance, particularly 1.421 and 1.258 Å. The difference between C_x–H and C_x–H_B^+ distances is probably caused by the steric effect between the reacting center and neighboring methyl moieties. Also, Al_1–O_2 and Al_1–O_3 bond lengths and O_2–$A1_1$–O_3 bond angle were found to be dependent on the types of the reaction centers (primary, secondary, or tertiary). The transition states for reactions at primary (ethane/1, propane/1, *i*-butane/1, and *n*-butane/1) and secondary (propane/2 and *n*-butane/2) carbons have Al_1–O_2 shorter than Al_1–O_3 and O_2–Al_1–O_3 angle around 90°. However, the bond variance for the reaction at the secondary carbon is more evident. For the reaction with *i*-butane/3, Al_1–O_2 is longer than Al_1–O_3 bond length and O_2–Al_1–O_3 bond angle of 89.6°. All of these behaviors could be ascribed to the steric effect between the reacting center and the alkane molecule.

3.2 Adsorption energy

Adsorption of the alkane molecule to zeolites represents an important step of the proton exchange reaction and was extensively investigated. Using PBE/DNP, adsorption energies of the ethane, propane, *i*-butane, and *n*-butane with various cluster models were calculated and the results are displayed in Fig. 4.

A non-negligible dependency of adsorption energies on the cluster size is observed. As the size increases, computed adsorption energies increase for all alkanes studied. The adsorption energy as predicted using the periodic model was up to 3–7 kcal/mol larger than that using the 5T model. Even with the 38T model, adsorption energies are still underestimated. Only with the 96T cluster an acceptable difference of ~1 kcal/mol between the cluster and the periodic calculations is achieved. The dependency of calculated values versus basis sets (DNP, SVP, and CBS) and methods (PBE and MP2) are displayed in Table 3. The CBS values were obtained using formulas provided in Sect. 2.3. In addition, the dispersion correction of adsorption energies (E_{disp}) as proposed by Grimme et al. [33] was calculated for various cluster sizes. For the periodic model, the equation as suggested by Kerber et al. [34] was used. This correction was used to adjust PBE/DNP values referred to as PBE-D (PBE/DNP + E_{disp}), and their values are given in Table 3. MP2 adsorption energies are found to be consistently larger than the PBE values. Improvement of basis set decreases their values. Interestingly, PBE-D values show good agreement with values obtained at MP2 level for all cluster sizes. However, even with the E_{disp} adjustment to PBE/DNP at periodic model computed adsorption energies will be too large as compared to experimental heats of adsorption. With DFT-D, Zimmerman et al. [14] arrived with similar observation for the adsorption of propane on ZSM-5. Thus, the discrepancy

Table 2 Selected parameters for the transition states of the proton exchange reaction of all alkanes in clusters 38T

Alkanes	Al_1–O_2	Al_1–O_3	Si_4–O_2–Al_1	Si_5–O_3–Al_1	O_2–Al_1–O_3	O_2–H_B^+	C_{1-3}–H_B^+	O_3–H	C_{1-3}–H	Al_1–C_{1-3}
Ethane	1.744	1.759	130.4°	132.5°	89.9°	1.453	1.282	1.426	1.289	3.663
Propane/1	1.744	1.758	130.4°	133.4°	90.1°	1.456	1.278	1.419	1.286	3.651
Propane/2	1.734	1.766	131.2°	130.8°	90.0°	1.546	1.251	1.422	1.338	3.723
i-Butane/1	1.746	1.755	130.8°	134.3°	90.6°	1.421	1.283	1.442	1.271	3.624
i-Butane/3	1.755	1.739	127.2°	133.8°	89.6°	1.518	1.421	1.611	1.258	3.855
n-Butane/1	1.746	1.757	130.2°	133.1°	90.1°	1.447	1.285	1.444	1.282	3.644
n-Butane/2	1.734	1.765	131.2°	131.3°	90.1°	1.546	1.249	1.421	1.331	3.712

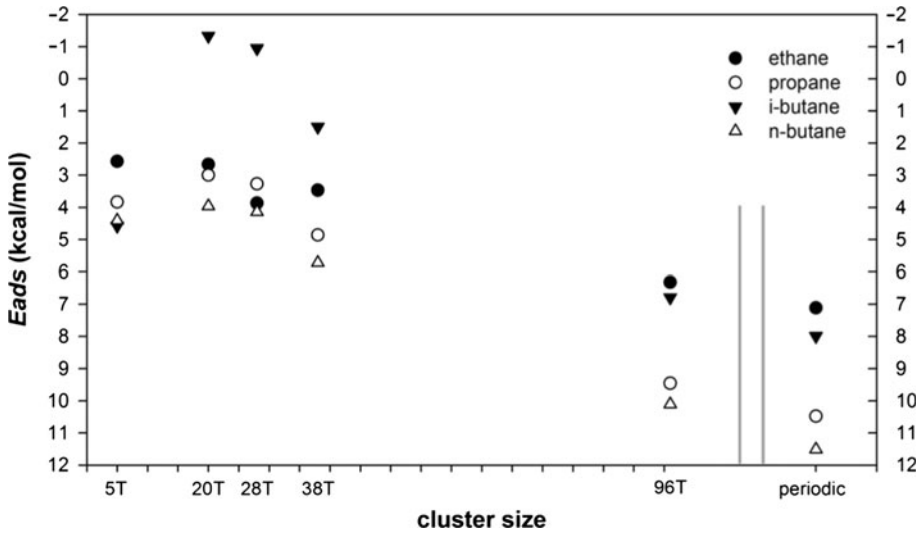

Fig. 4 Adsorption energy (E_{ads}) of C2–C4 alkanes in ZSM-5 as function of cluster size calculated using PBE/DNP

Table 3 Adsorption energies (E_{ads}) in kcal/mol of ethane, propane, *i*-butane, and *n*-butane on ZSM-5 computed using PBE/DNP, PBE/CBS, MP2/SVP, MP2/CBS, and PBE-D (PBE/DNP + E_{disp}) with 5T, 28T, 38T, and P in comparison with experimental enthalpies of adsorption

Alkanes	E_{ads}									Experiments
	PBE/DNP		PBE/CBS	MP2/SVP		MP2/CBS	PBE-D			
	38T	P	38T	5T	28T	5T	5T	28T	P	
Ethane	3.5	7.1	1.0	4.7	13.1	2.9	5.1	13.4	18.0	7.3 [36], 6.9 [37]
Propane	4.9	10.5	1.4	8.5	16.5	6.2	9.1	16.5	24.7	10.2 [4], 9.5 [38], 10.9 [39]
i-Butane	1.5	8.0	−3.2	8.8	18.6	6.6	10.0	18.4	26.7	11.6 [40], 12.4 [39]
n-Butane	5.7	11.5	1.1	9.7	19.2	7.4	10.5	19.1	29.8	14.7 [4], 11.9 [38], 14.3 [5]

should come from the overestimation of dispersion energy from the Grimme et al. [33] and Kerber et al. [34] formulae as well as from the MP2 calculations. De Moor et al. [35] using QM-Pot(MP2//B3LYP) have shown that adsorption enthalpies of *n*-alkanes (C2–C8) in H-FAU, H-BEA, H-MOR, and H-ZSM-5 at 341, 370, and 400 K are nearly independent of temperature and adsorption enthalpies at 373, 773, and 1139 K slightly depend on the temperature. In the subsequent discussion, we will use the experimental enthalpies of adsorption for calculations of apparent reaction barriers in the later section without worrying about their temperature dependency.

3.3 Proton exchange barrier

3.3.1 Cluster-size dependency

The effect of cluster size on reaction barriers of the proton exchange reactions discussed in this work is displayed in Fig. 5 where activation energies computed using PBE/DNP are plotted against the cluster size, that is, 5T, 20T, 28T, 38T, 96T, and P models. For all alkanes, proton exchange barriers are reduced by around 5 and 10 kcal/mol when expanding from 5T to 38T and from 38T to 96T, respectively. However, a reduction of less than 2 kcal/mol is observed when the model was further extended to periodic boundary conditions. It appears that performing calculations using the 38T cluster model is not sufficient to render the cluster-size effect, since the largest decrease of the predicted reaction barrier was observed when expanding from 38T to P model. The cluster-size effect becomes minimal when including all atoms in the unit cell (96T).

Table 4 displays theoretical (intrinsic) activation energies (in kcal/mol) for proton exchange reactions of C2–C4 alkanes in ZSM-5 compared with previous DFT calculations using the 3T cluster model [15–18]. Our PBE/DNP activation barriers for 5T clusters are in a relatively good agreement with the other theoretical results at 3T level. However, with the periodic model, activation energies for proton exchange reactions of C2–C4 alkanes in ZSM-5 are strongly reduced and range between 12.1 (ethane) and 28.4 (*i*-butane/3) kcal/mol. It is evident that predicted activation energies of all alkanes reduce drastically with the increment of the cluster size. The reduction is in the range of 10 (butane/1) to 20 (ethane) kcal/mol. This large reduction of activation energy has also been observed by Sauer et al. [41] who performed theoretical calculations for methylation reactions of alkanes in ZSM-5. Thus, the cluster-size

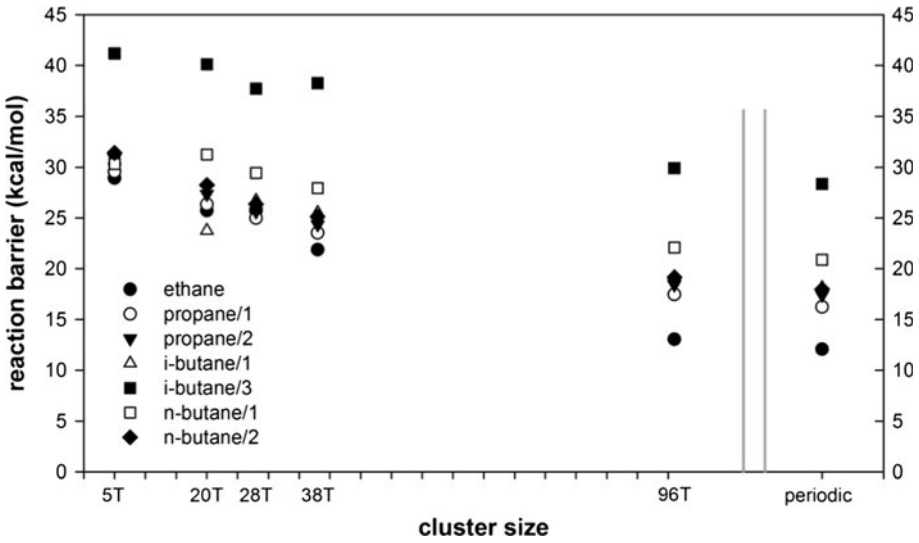

Fig. 5 Reaction barriers (intrinsic activation energies) of proton exchange reactions of C2–C4 alkanes in ZSM-5 calculated using PBE/DNP as a function of cluster size

Table 4 Intrinsic activation energies (in kcal/mol) of the proton exchange reactions for C2–C4 alkanes in ZSM-5 obtained using PBE/DNP for 5T, and P models in comparison with previous DFT calculations using the 3T model

Alkanes	5T	P	Previous DFT work (3T)
Ethane	28.9	12.1	28.2 [16], 32.3 [15], 31.0 [17]
Propane/1	29.6	16.3	32.2 [15], 30.4[17]
Propane/2	30.9	17.4	33.3 [15], 29.8 [17]
i-Butane/1	32.6	18.1	32.3 [15], 29.4[18]
i-Butane/3	41.2	28.4	36.2 [15], 29.9 [18]
n-Butane/1	30.3	20.9	29.9 [17]
n-Butane/2	31.4	18.0	28.3 [17]

effect is non-negligible and crucial. These reaction barriers at periodic model for the proton exchange reactions of C2–C4 alkanes in ZSM-5 are quite different from those in chabazite which were reported by Bučko et al. [20]. Unlike our predictions, proton exchange barriers in chabazite are larger and showed no linear dependency with the alkane chain length. There is the chain-length dependency with increment of ~4 kcal/mol. This is in agreement with experiments where the increments of 2–3 kcal/mol were reported [39, 42, 43]. The smaller cavity of chabazite as compared to ZSM-5 might be a reason for a difference in the chain-length dependency between 2 zeolites.

3.3.2 *Basis set dependency*

Table 5 lists reaction barriers for proton exchange reactions of C2–C4 alkanes for 5T and 38T cluster models calculated using RI-PBE with SVP and/or TZVPPP basis sets, respectively. The values at CBS limit were obtained using the procedure as described in Sect. 2.3. It appears that computed reaction barriers for all proton exchange reaction increase with the improvement of the basis set. For the 5T model, when changing from SVP to TZVPPP, the activation energies were raised between 1.9 and 4.6 kcal/mol. The increment from TZVPPP to CBS limit is smaller, only 0.1–0.4 kcal/mol. For the 38T model, computed reaction barriers increase between 2.5–3.6 (SVP to TZVPPP) and 0.2–0.3 kcal/mol (TZVPPP to CBS), respectively. It could be noticed that there is a smaller increase of the activation energy due to the improvement of the basis set for the larger 38T cluster. This is probably because of the more extended availability of functions in the larger cluster that makes the basis set more complete. Thus, for DFT calculations with PBE functional, the effect of basis set has a positive contribution to the obtained activation energies.

3.3.3 *Effect of the level of electron correlation*

Activation energies could be better estimated by incorporation of electron correlation. Generally, this could be achieved by performing MP2 calculations. However, the effect of the electron correlation is, as well, cluster-size dependent as pointed out by Sauer et al. [41]. Table 6 shows the reaction barriers of the proton exchange reaction of C2–C4 alkanes in ZSM-5 computed with the RI-MP2/SVP method for the 5T, 28T, and 38T models in comparison with previous MP2 calculations on 3T model. Our MP2 calculations gave activation energies in the same range as those reported by previous work. From Table 6, the cluster-size dependency as previously observed in PBE/DNP calculations (Fig. 5) is evident. The decrement of the activation energies from 2.9 (ethane) to 6.7 (*i*-butane/1) kcal/mol was obtained, and larger values of activation energies as compared to DFT calculations were reported.

Table 5 Reaction barriers (in kcal/mol) of proton exchange reactions of C2–C4 alkanes on 5T and 38T cluster model computed using RI-PBE with SVP and TZVPPP basis sets, and CBS limit

Alkanes	RI-PBE/SVP		RI-PBE/TZVPPP		RI-PBE/CBS limit	
	5T	38T	5T	38T	5T	38T
Ethane	24.4	20.2	28.4	22.8	28.7	23.0
Propane/1	26.9	22.1	29.2	24.6	29.4	24.8
Propane/2	27.4	22.6	30.5	25.3	30.8	25.5
i-Butane/1	26.6	23.0	30.2	26.6	30.4	26.9
i-Butane/3	36.1	35.5	40.7	39.1	41.1	39.3
n-Butane/1	28.0	26.0	29.9	29.1	30.0	29.3
n-Butane/2	28.3	23.5	31.1	26.3	31.3	26.5

To obtain accurate prediction of reaction barriers for the proton exchange reaction of C2–C4 in ZSM-5, it would be useful to perform MP2 calculations for the periodic model. However, such MP2 calculations are extremely costly and not feasible. From our calculations on adsorption energies, we found a good relation between dispersion energy computed using Grimme et al. [33] formula and the MP2–PBE energy difference. Therefore, dispersion interactions were adopted to adjust PBE activation energies. Table 7 shows the contribution of dispersion interactions to activation energy ($\Delta E^{\ddagger}_{\text{disp}}$) for proton exchange reactions of C2–C4 alkanes in ZSM-5 as a function of cluster size in comparison with MP2–PBE activation energy differences for 5T, 28T, and 38T model. The MP2–PBE activation energy differences could be assigned to a different treatment of electron correlation.

As expected, $\Delta E^{\ddagger}_{\text{disp}}$ are negative and cluster-size dependent for all alkanes. For all alkanes, $\Delta E^{\ddagger}_{\text{disp}}$ for 38T and 96T clusters are appeared to be similar, which suggests the convergence of $\Delta E^{\ddagger}_{\text{disp}}$ at 38T model. We found that $\Delta E^{\ddagger}_{\text{disp}}$ at P remains the same as that at 96T. The dispersion correction seems to already converge at 96T. However, E_{disp} (of related species) at 96T and P are just around 3–4 kcal/mol different. In addition, the effect of dispersion interactions depends on the alkane molecule. The effect is larger (more negative) for larger alkane. The dispersion interactions are also governed by the shape of the TS complex. For example, the effect of dispersion interactions on the proton exchange barrier of *i*-butane is larger at the tertiary than the primary position.

Table 6 Reaction barriers (in kcal/mol) of proton exchange reactions of C2–C4 alkanes computed using RI-MP2/SVP on 5T, 28T, and 38T cluster models in comparison with previous MP2/6-31G**//HF/6-31G** calculations on 3T model

Alkanes	5T	28T	38T	Previous work (3T)
Ethane	32.5	32.4	29.6	31.4 [15]
Propane/1	35.8	30.5	29.2	30.6 [15]
Propane/2	34.8	32.3	29.1	30.6 [15]
i-Butane/1	34.8	32.5	28.1	29.8 [15]
i-Butane/3	42.9	42.3	39.2	31.5 [15]
n-Butane/1	37.0	29.2	31.2	–
n-Butane/2	35.8	29.2	30.0	–

MP2–PBE activation energy differences are positive and, similarly to $\Delta E^{\ddagger}_{\text{disp}}$, also cluster-size dependent. However, the difference between MP2–PBE activation energy differences and $\Delta E^{\ddagger}_{\text{disp}}$ does not depend on the cluster size. For example, the differences in kcal/mol are −7.8 at 5T, −7.4 at 28T, and −8.1 at 38T for ethane, and −7.4 at 5T, −7.3 at 28T, and −7.3 at 38T for *i*-butane/1. Knowing this, such constant difference or "E_{adj}" can be used to adjust $\Delta E^{\ddagger}_{\text{disp}}$ for MP2–PBE activation energy differences at a larger cluster size in a following way

$$\left[\Delta E^{\ddagger}_{\text{disp}}\right]_c = \left[\Delta E^{\ddagger}_{\text{MP2}}\right]_c - \left[\Delta E^{\ddagger}_{\text{DFT}}\right]_c + E_{\text{adj}} \quad (6)$$

This is somehow in accordance with the suggestion by Sauer et al. [34, 41].

3.3.4 Zero-point-energy correction

The zero-point-energy (ZPE) corrections were performed using RI-PBE/SVP for the 5T, 20T, 28T, and 38T cluster models. Their values as a function of cluster size are illustrated in Fig. 6. According to Fig. 6, the ZPE correction has a negative contribution to the computed reaction barrier and the values vary with the cluster size. However, the size dependency seems to converge very fast. For the proton exchange reactions of C2–C4 alkanes in ZSM-5, the ZPE correction already converges at 28T model. ZPEs for 38T model are ranging between −1.6 and −2.5 kcal/mol.

3.3.5 Apparent reaction barriers

In previous sections, it has been shown that apart from the cluster size, other effects such as basis set and level of electron correlation are non-negligible. The augmentation of larger basis sets and electron correlation raises values of predicted proton exchange barriers. However, it is hard to

Table 7 RI-MP2/SVP and PBE/DNP activation energy differences in kcal/mol for proton exchange reaction of C2–C4 alkanes in ZSM-5 for 5T, 28T, and 38T cluster model and dispersion contributions ($\Delta E^{\ddagger}_{\text{disp}}$) in kcal/mol for 5T, 20T, 28T, 38T, 96T, and periodic models

Alkanes	$\Delta E^{\ddagger}$(RI-MP2/SVP) − $\Delta E^{\ddagger}$(PBE/DNP) 5T	$\Delta E^{\ddagger}$(RI-MP2/SVP) − $\Delta E^{\ddagger}$(PBE/DNP) 28T	$\Delta E^{\ddagger}$(RI-MP2/SVP) − $\Delta E^{\ddagger}$(PBE/DNP) 38T	$\Delta E^{\ddagger}_{\text{disp}}$					
				5T	20T	28T	38T	96T	P
Ethane	3.6	6.7	7.7	−4.2	0.0	−0.7	−0.4	−0.4	−0.4
Propane/1	6.2	5.5	5.6	−1.7	−2.1	−1.9	−2.4	−2.1	−2.1
Propane/2	3.9	6.0	4.8	−3.1	−1.0	−0.3	−2.2	−2.1	−2.1
i-Butane/1	4.2	5.8	2.6	−3.2	2.9	−1.5	−4.7	−4.1	−4.1
i-Butane/3	1.7	4.6	0.9	−5.9	−2.8	−2.7	−6.0	−5.7	−5.7
n-Butane/1	6.7	−0.2	3.3	−1.6	−7.1	−6.8	−5.0	−4.6	−4.6
n-Butane/2	4.4	2.8	4.8	−3.0	−3.9	−3.6	−2.8	−2.6	−2.6

accommodate all of these effects without resourcing to enormous amounts of computation time. Here, an extrapolated scheme where effects of electron correlation and basis set could be addressed with modest computing efforts was proposed. For periodic model, the extrapolated reaction barrier, $\Delta E^{\ddagger}_{\text{ex}}$, is

$$\left[\Delta E^{\ddagger}_{\text{ex}}\right]_p = \left[\Delta E^{\ddagger}_{\text{DFT}}\right]_P + \left[\Delta E^{\ddagger}_{\text{disp}}\right]_{96T} + \left[\Delta E^{\ddagger}_{\text{basis}}\right]_{38T} - E_{\text{adj}}. \quad (7)$$

The $[\Delta E^{\neq}_{\text{basis}}]_{38T}$ values were obtained from $\Delta E^{\neq}$(38T, PBE/CBS) – $\Delta E^{\neq}$(38T, PBE/DNP). The proposed extrapolation scheme given by Eq. (7) is in the same light as it has been previously suggested by Sauer et al. [41] Extrapolated proton exchange barriers (intrinsic) are ranging from 20.9 (ethane) to 30.5 (*i*-butane/3) kcal/mol, and their values as well as the decomposition energies are shown in Table 8.

The apparent reaction barrier ($\Delta E^{\ddagger}_{\text{app}}$) was calculated from $\Delta E^{\ddagger}_{\text{ex}}$ plus the adsorption enthalpies from experiments given in Table 3. The apparent reaction barriers and the apparent reaction barrier plus ZPE correction for proton exchange reaction of C2–C4 alkanes in ZSM-5 are also given in Table 8. The ZPE correction was computed using RI-PBE/SVP for the 38T cluster model. $\Delta E^{\ddagger}_{\text{app}}$ + ZPE values range around 9–12 kcal/mol for all proton exchange reactions with exception of *i*-butane/3, which has the barrier of 17.4 kcal/mol. This different behavior of *i*-butane/3 is possibly due to its shape. While other alkanes possess a linear or quasi-linear shape, *i*-butane/3 has a globular-like structure. Apparent enthalpies, entropies, and Gibbs free energies of activation for the proton exchange reaction of C2–C4 alkanes in ZSM-5 at 500 K were calculated and are listed in Table 9.

Statistical mechanics models were applied for computations of translation, rotation, vibration (with vibration frequency from 38T model), and electronic contributions to enthalpy and entropy [44]. For the enthalpy, the electronic contribution ($\Delta H^{\ddagger}_{\text{elec}}$) was determined from apparent reaction barrier with ZPE correction. Entropies of activation are negative and have values between 40.6 (ethane) and 47.6 (*n*-butane/1) cal $K^{-1}mol^{-1}$ for the proton exchange reaction in ZSM-5. From the Arrhenius equation, the entropy term contributes to the prefactor [35] and, thus, it slows down the proton exchange rate. Apparent Gibbs energies of activation at 500 K are in the range of 30.3 (ethane) to 40.6 (*i*-butane/3) kcal/mol.

Computed $\Delta H^{\ddagger}$ values are compared in Table 9 with experimental results obtained from Arrhenius plots. In most cases, our best values, including extrapolation techniques are significantly too small. Interestingly, the computed barriers obtained from small cluster sizes agree quite well with experiment. However, as our investigations show, this good agreement is fortuitous. It should be noticed that the works of Hansen et al. [46] on alkylation of benzene and Tuma et al. [47] on deprotonation of a tert-butyl cation using similar computational scheme to ours showed good results compared with experiments. More investigations will be needed to explain this discrepancy.

3.4 Regioselectivity

Performing calculations in chabazite, Bučko et al. [20] suggested the entropy contribution to be crucial for describing the regioselectivity of the proton exchange reaction [13]. This is because in chabazite, the potential energy for proton exchange reactions is the same for all reactions. Unlike the report of Bučko et al. [20], we could observe the regioselectivity of the proton exchange reaction when consider either the entropy contribution or enthalpy. However, the direction is different. Considering only the entropy contribution, the proton exchange reaction for all alkanes proceeds faster at the primary position than at the secondary and tertiary positions. However, the enthalpies of activation predict the proton exchange reaction to proceed faster at the primary position for *i*-butane but at the secondary position for propane and *n*-butane. At

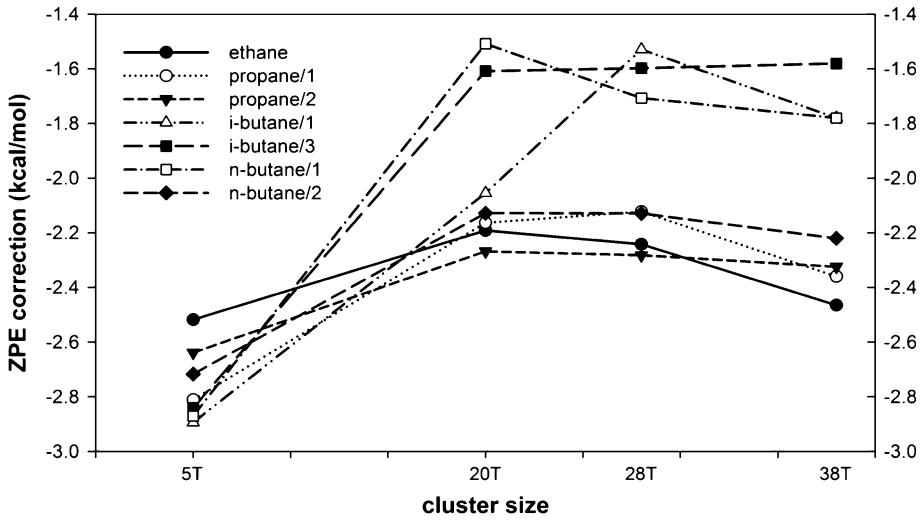

Fig. 6 ZPE corrections calculated using RI-PBE/SVP for reaction barriers of proton exchange reactions of C2–C4 alkanes in ZSM-5 as a function of cluster size

Table 8 Extrapolated intrinsic ($\Delta E^{\ddagger}_{ex}$) and apparent ($\Delta E^{\ddagger}_{app}$) reaction barriers of proton exchange reactions of C2–C4 alkanes in ZSM-5 as well as $\Delta E^{\ddagger}_{disp} - E_{adj}$, basis set ($\Delta E^{\ddagger}_{basis}$), and ZPE in comparison with experiments (all in kcal/mol)

	$\Delta E^{\ddagger}_{P}$	$\Delta E^{\ddagger}_{disp} - E_{adj}$	$\Delta E^{\ddagger}_{basis}$	$\Delta E^{\ddagger}_{ex}$	$\Delta E^{\ddagger}_{app}$	ZPE	$\Delta E^{\ddagger}_{app}$ + ZPE
Ethane	12.1	7.7	1.1	**20.9**	13.6	−2.5	**11.1**
Propane/1	16.3	5.8	1.3	**23.3**	13.1	−2.4	**10.8**
Propane/2	17.4	4.8	1.1	**23.3**	13.1	−2.3	**10.8**
i-Butane/1	18.1	3.2	1.4	**22.7**	11.1	−1.8	**9.3**
i-Butane/3	28.4	1.1	1.0	**30.5**	18.9	−1.6	**17.4**
n-Butane/1	20.9	3.6	1.4	**25.8**	13.9	−1.8	**12.1**
n-Butane/2	18.0	5.0	1.4	**24.4**	12.5	−2.2	**10.8**

Bold values indicate that they result from summation of the previous columns

Table 9 Apparent reaction enthalpies ($\Delta H^{\ddagger}$), entropy contributions ($T\Delta S^{\ddagger}$), and Gibbs free energies of activation ($\Delta G^{\ddagger}$) (in kcal/mol) for proton exchange reactions of C2–C4 alkanes in ZSM-5 at 500 K

	$\Delta H^{\ddagger}$	$-T\Delta S^{\ddagger}$	$\Delta G^{\ddagger}$	Experiments (Arrhenius barriers)
Ethane	12.3	18.0	30.3	
Propane/1	12.2	18.8	31.0	25.7 ± 1.6 [6], 25.5 ± 2.4 [7]
Propane/2	12.5	19.1	31.5	27.8 ± 1.6 [6], 29.7 ± 1.4 [7]
i-Butane/1	11.1	20.9	32.0	12.0 ± 0.5 [12], 13.6 [45]
i-Butane/3	19.8	20.8	40.6	
n-Butane/1	13.9	21.7	35.6	19.0 [4, 8], 20.2 [5], 27.5 ± 7.2 [9]
n-Butane/2	12.1	19.6	31.7	28.9 ± 8.4 [9]

higher temperature, the entropy term will become dominant and govern the direction of the Gibbs energy of activation. This does not mean that the entropy dictates the direction of regioselectivity. The activation Gibbs free energy for *i*-butane/3 proton exchange is almost 8 kcal/mol larger than *i*-butane/1, which suggests the proton exchange reaction at the tertiary position as impossible for *i*-butane. However, the entropy contribution for *i*-butatne/3 is the same as for *i*-butane/1. Therefore, Gibbs free energy of activation should be rather considered when addressing the regioselectivity. The data in Table 9 are the values at 500 K. To compare with experiments, we determined Gibbs free energies of activation for the proton exchange of propane in ZSM-5 at 553 K. For propane/1 and propane/2 reactions, Gibbs free energies of activation are 35.9 and 36.3 kcal/mol, respectively. Using transition-state theory [44], $k = \frac{k_B T}{h} e^{\Delta G^{\ddagger}/RT}$ where k is the rate constant, the proton transfer rate at the primary position is found to be 1.4 times faster than at the tertiary position in good agreement with experiments (1.5 times) [7]. Thus, the regioselectivity of the proton exchange reaction of alkanes in ZSM-5 is well predicted.

4 Conclusion

The TS structures for the reactions on the primary and secondary carbon have shorter or almost equivalent C_x–H_B^+ and C_1–H distances ($\sim$1.3 Å), while for the tertiary carbon,

the C_x–H_B^+ distance is longer (1.4 Å). Steric effects are used to describe this behavior. The TS structures reflect the stability of the TS complex and hence the activation energies for the proton transfer of alkanes in ZSM-5. The effect of cluster size reduces the activation energy of proton exchange reactions of C2–C4 alkanes in ZSM-5 computed when using small cluster model by 20 kcal/mol. For ZSM-5, the cluster-size effect is converged at 96T model where the ZSM-5 cavity is well-represented. The chain-length dependency of the proton exchange barrier of alkanes in ZSM-5 could be predicted. Therefore, it is important to choose a model that could describe the cavity structure of zeolites. Contributions representing effects of level of basis set and electron correlation on computed activation energies could be as high as +8 kcal/mol. An extrapolated scheme that includes effects of cluster size, basis set, and electron correlation for the estimation of proton exchange barrier in ZSM-5 has been proposed. Computed energy barriers based on our most extended extrapolations are found to be significantly too low as compared to experiment data. The origin of this discrepancy is still unclear. The Gibbs free energies of activation are used to predict the regioselectivity for the proton exchange reaction of propane, *n*-butane, and *i*-butane. The preference of the primary position to other position is observed. From Gibbs free energies of activation at 553 K, the rate of proton transfer for propane in ZSM-5 is 1.4 times faster at the primary position than at the secondary position, in agreement with experiment.

Acknowledgments Thanks to the Office of the Higher Education Commission, Ministry of Education, Thailand for supporting Ms. Kanjarat Sukrat under the program "Strategic Scholarships for Frontier Research Network for the Joint Ph.D. Program Thai Doctoral degree." Special thanks to the Radchadapisek Sompot Endowment grants of Chulalongkorn University, The National Research University Project of CHE, and the Ratchadapisek Somphot Endowment Fund (AM1078I). The authors are also grateful to the Computational Chemistry Unit Cell, Faculty of Science, Chulalongkorn University, the Institute for Theoretical Chemistry, University of Vienna, the Vienna Scientific Cluster (VSC-1, project No. 70055), and to National Electronics and Computer Technology Center (NECTEC), Thailand, for providing research facilities, software packages, and computing times. The authors are finally grateful for financial support from the Austrian Sciences Fund (project P20893-N19), and the German Research Foundation (DFG), priority program SPP 1315, projects No. GE 1676/1-1 and SCHA849/8-1. Support was also provided by the Robert A. Welch Foundation under Grant No. D-0005.

References

1. Vermeiren W, Gilson JP (2009) Impact of zeolites on the petroleum and petrochemical industry. Top Catal 52(9):1131–1161
2. The intelligence report: business shift in the global catalytic process industries 2005–2011. The Catalyst Group Resources, Inc, May 2006
3. World catalysts. The Freedonia Group, Inc, Jan 2007
4. Narbeshuber TF, Vinek H, Lercher JA (1995) Monomolecular conversion of light alkanes over H-ZSM-5. J Catal 157(2):388–395
5. Lercher JA, Santen RA, Vinek H (1994) Carbonium ion formation in zeolite catalysis. Catal Lett 27(1):91–96
6. Stepanov A, Ernst H, Freude D (1998) In situ ^{1}H MAS NMR studies of the H/D exchange of deuterated propane adsorbed on zeolite H-ZSM-5. Catal Lett 54(1):1–4
7. Arzumanov SS, Reshetnikov SI, Stepanov AG, Parmon VN, Freude D (2005) In Situ ^{1}H and ^{13}C MAS NMR kinetic study of the mechanism of H/D exchange for propane on zeolite H-ZSM-5. J Phys Chem B 109(42):19748–19757. doi:10.1021/jp054037n
8. Narbeshuber TF, Stockenhuber M, Brait A, Seshan K, Lercher JA (1996) Hydrogen/deuterium exchange during *n*-butane conversion on H-ZSM-5. J Catal 160(2):183–189
9. Arzumanov SS, Stepanov AG, Freude D (2008) Kinetics of H/D exchange for *n*-butane on zeolite H-ZSM-5 studied with ^{1}H MAS NMR in situ. J Phys Chem C 112(31):11869–11874. doi:10.1021/jp802162h
10. Zheng A, Deng F, Liu S-B (2011) Regioselectivity of carbonium ion transition states in zeolites. Catal Today 164(1):40–45
11. Kramer GJ, van Santen RA, Emeis CA, Nowak AK (1993) Understanding the acid behaviour of zeolites from theory and experiment. Nature 363(6429):529–531
12. Sommer J, Habermacher D, Jost R, Sassi A, Stepanov AG, Luzgin MV, Freude D, Ernst H, Martens J (1999) Activation of small alkanes on solid acids. An H/D exchange study by liquid and solid-state NMR: the activation energy and the inhibiting effect of carbon monoxide. J Catal 181(2):265–270
13. Stepanov AG, Arzumanov SS, Luzgin MV, Ernst H, Freude D, Parmon VN (2005) In situ ^{1}H and ^{13}C MAS NMR study of the mechanism of H/D exchange for deuterated propane adsorbed on H-ZSM-5. J Catal 235(1):221–228
14. Zimmerman PM, Head-Gordon M, Bell AT (2011) Selection and validation of charge and Lennard-Jones parameters for QM/MM simulations of hydrocarbon interactions with zeolites. J Chem Theory Comput 7(6):1695–1703. doi:10.1021/ct2001655
15. Esteves PM, Nascimento MAC, Mota CJA (1999) Reactivity of alkanes on zeolites: a theoretical ab initio study of the H/H exchange. J Phys Chem B 103(47):10417–10420. doi:10.1021/jp990555k
16. Blaszkowski SR, Nascimento MAC, van Santen RA (1996) Activation of C–H and C–C bonds by an acidic zeolite: a density functional study. J Phys Chem 100(9):3463–3472. doi:10.1021/jp9523231
17. Zheng X, Blowers P (2005) A computational study of alkane hydrogen-exchange reactions on zeolites. J Mol Catal A: Chem 242(1–2):18–25
18. Zheng X, Blowers P (2006) Reactivity of isobutane on zeolites: a first principles study. J Phys Chem A 110(7):2455–2460. doi:10.1021/jp056707v
19. Tuma C, Sauer J (2006) Treating dispersion effects in extended systems by hybrid MP2: DFT calculations–protonation of isobutene in zeolite ferrierite. Phys Chem Chem Phys 8(34):3955–3965
20. Bučko T, Benco L, Hafner J, Ángyán JG (2007) Proton exchange of small hydrocarbons over acidic chabazite: Ab initio study of entropic effects. J Catal 250(1):171–183
21. Delley B (2000) From molecules to solids with the DMol3 approach. J Chem Phys 113(18):7756–7764
22. Ahlrichs R, Bär M, Häser M, Horn H, Kölmel C (1989) Electronic structure calculations on workstation computers: the program system turbomole. Chem Phys Lett 162(3):165–169
23. Truhlar DG (1998) Basis-set extrapolation. Chem Phys Lett 294(1–3):45–48

24. Hohenberg P, Kohn W (1964) Inhomogeneous electron gas. Phys Rev 136(3B):B864–B871
25. Perdew JP, Burke K, Ernzerhof M (1996) Generalized gradient approximation made simple. Phys Rev Lett 77(18):3865–3868
26. Schafer A, Horn H, Ahlrichs R (1992) Fully optimized contracted Gaussian basis sets for atoms Li to Kr. J Chem Phys 97(4):2571–2577
27. Schafer A, Huber C, Ahlrichs R (1994) Fully optimized contracted Gaussian basis sets of triple zeta valence quality for atoms Li to Kr. J Chem Phys 100(8):5829–5835
28. Eichkorn K, Weigend F, Treutler O, Ahlrichs R (1997) Auxiliary basis sets for main row atoms and transition metals and their use to approximate Coulomb potentials. Theor Chem Acc 97(1):119–124
29. Delley B (1990) An all-electron numerical method for solving the local density functional for polyatomic molecules. J Chem Phys 92(1):508–517
30. Delley B (1991) Analytic energy derivatives in the numerical local-density-functional approach. J Chem Phys 94(11):7245–7250
31. Delley B (1996) Fast calculation of electrostatics in crystals and large molecules. J Phys Chem 100(15):6107–6110. doi:10.1021/jp952713n
32. Helgaker T, Klopper W, Koch H, Noga J (1997) Basis-set convergence of correlated calculations on water. J Chem Phys 106(23):9639–9646
33. Grimme S (2006) Semiempirical GGA-type density functional constructed with a long-range dispersion correction. J Comput Chem 27(15):1787–1799
34. Kerber T, Sierka M, Sauer J (2008) Application of semiempirical long-range dispersion corrections to periodic systems in density functional theory. J Comput Chem 29(13):2088–2097. doi:10.1002/jcc.21069
35. De Moor BA, M-F Reyniers, Gobin OC, Lercher JA, Marin GB (2010) Adsorption of C2–C8 *n*-alkanes in zeolites. J Phys Chem C 115(4):1204–1219. doi:10.1021/jp106536m
36. Hampson JA, Rees LVC (1993) Adsorption of ethane and propane in silicalite-1 and zeolite NaY: determination of single components, mixture and partial adsorption data using an isosteric system. J Chem Soc, Faraday Trans 89:3169–3176
37. Stach H, Fiedler K, Janchen J (1993) Correlation between initial heats of adsorption and structural parameters of molecular sieves with different chemical composition—a calorimetric study. Pure Appl Chem 65(10):2193–2200
38. Anderson BG, Schumacher RR, van Duren R, Singh AP, van Santen RA (2002) An attempt to predict the optimum zeolite-based catalyst for selective cracking of naphtha-range hydrocarbons to light olefins. J Mol Catal A: Chem 181(1–2):291–301
39. Eder F, Stockenhuber M, Lercher JA (1997) Bronsted acid site and pore controlled siting of alkane sorption in acidic molecular sieves. J Phys Chem B 101(27):5414–5419. doi:10.1021/jp9706487
40. Yanping S, Brown TC (2000) Kinetics of isobutane dehydrogenation and cracking over HZSM-5 at low pressures. J Catal 194(2):301–308
41. Svelle S, Tuma C, Rozanska X, Kerber T, Sauer J (2009) Quantum chemical modeling of zeolite-catalyzed methylation reactions: toward chemical accuracy for barriers. J Am Chem Soc 131(2):816–825. doi:10.1021/ja807695p
42. Eder F, Lercher JA (1997) Alkane sorption in molecular sieves: the contribution of ordering, intermolecular interactions, and sorption on Brønsted acid sites. Zeolites 18(1):75–81
43. Eder F, Lercher JA (1997) On the role of the pore size and tortuosity for sorption of alkanes in molecular sieves. J Phys Chem B 101(8):1273–1278. doi:10.1021/jp961816i
44. Jensen F (2006) Introduction to computational chemistry, 2nd edn. Wiley, Chichester
45. Truitt MJ, Toporek SS, Rovira-Truitt R, White JL (2006) Alkane C–H bond activation in zeolites: evidence for direct protium exchange. J Am Chem Soc 128(6):1847–1852. doi:10.1021/ja0558802
46. Hansen N, Kerber T, Sauer J, Bell AT, Keil FJ (2010) Quantum chemical modeling of benzene ethylation over H-ZSM-5 approaching chemical accuracy: a hybrid MP2: DFT study. J Am Chem Soc 132(33):11525–11538. doi:10.1021/ja102261m
47. Tuma C, Kerber T, Sauer J (2010) The tert-butyl cation in H-zeolites: deprotonation to isobutene and conversion into surface alkoxides. Angew Chem Int Ed 49(27):4678–4680. doi:10.1002/anie.200907015